Investigation of Atomistic-Scale Thin-Film Evaporation

Kimia Montazeri, Shiwei Zhang, Mohammad Javad Abdolhosseini Qomi, Yoonjin Won*
University of California Irvine
Irvine, California, USA, 92617
* Email: won@uci.edu

ABSTRACT

Thermal cooling technologies that dissipate high heat levels from high-performance electronic devices require the enhancement of evaporating performances. Nanoscale surfaces are often employed to promote evaporating performances by enabling thin-film evaporation. Such nanoscale surfaces lead to varying thin-film thicknesses and intertwined physics associated with solid-liquid contact regions and liquid-vapor phase change processes. Despite numerous efforts using continuum theory or experiments, the understanding of interfacial phenomena during the evaporating phase change at the atomistic level still remains challenging. Molecular-level simulation receives significant attention for identifying surface effects on evaporating performance by capturing the atomistic level physics of thin-film evaporation.

In this study, we investigate nanometer-thin-film evaporation on flat surfaces by performing atomistic-level calculations. For this, we study molecular dynamics simulation methods that are capable of simulating interatomic forces between particles and corresponding particle behaviors. By using appropriate interatomic potentials, simulation models estimate how liquid-solid contact lines form on flat substrates and how liquid-vapor interfaces evolve. These calculations will provide a correlation among thin-film thicknesses, liquid-vapor interfaces, and evaporation rates. The understanding will enable us to classify effective and non-effective evaporating regimes along the meniscus during thin-film evaporation, enabling better design of microfluidic evaporators.

KEYWORDS: molecular dynamics, thin-film evaporation, surface tension, meniscus formation

NOMENCLATURE

A	surface area, Å^2
C	scaling factor
CA	contact angle, ^{o}
F	degrees of freedom
k	Boltzmann constant, J/K
K_e	kinetic energy
m	mass, g
m''	evaporation rate, kg/m^{2}s
N	number of molecules
T	temperature
r	interparticle distance, Å
t	time, s

Greek symbols

δ	thickness, nm
δ_o	original thickness, nm
ϵ	depth of energy well, eV
ρ	density, kg/m^3
σ	length scale, nm
Φ	potential, eV

Subscripts

l	liquid
lv	liquid-vapor interface
H_2O	water
o	initial

INTRODUCTION

Investigating liquid-vapor interfaces and their behaviors in equilibrium or during phase change processes such as evaporation and condensation has been the subject of numerous experimental and theoretical studies. The interest towards interface characteristics [1-6] has been critical because of the importance of two phase systems related to complex phase change physics. Since the development of the Hertz-Knudsen-Schrage equation to determine the evaporation flux, numerous efforts have been conducted in order to predict the evaporation rates and heat fluxes at the interface between two phases [7]. In addition to the complex nature of phase change, water is known to have a strong hydrogen bond network, leading to dynamic behavior in nanoscale features, which makes it more difficult to measure. Extensive studies have investigated phase change physics based on mechanical or thermodynamic expressions. However, detailed understanding of the inherently multiscale physics is still lacking. Employing proper models that are capable of simulating atomistic level interactions and interfacial dynamics is essential in order to provide better knowledge of phase change processes. Molecular dynamics simulation will allow us to compute statistical mechanics, enabling us to gain a precise understanding of the complex phenomena during phase change.

In this work, we first develop molecular dynamics calculations to identify the surfaces' role in improving wetting and evaporation physics [6-7-8]. Then, we address the research question of how film thickness of thin liquid film on varying solid surfaces determines phase change phenomena and

corresponding evaporation rate [6]. Careful understanding of the engineered surfaces' effects on multiphase transport phenomena will pave the way for future materials and system designs for enhanced phase change heat and mass transfer.

SURFACE INTERFACE CHARACTERIZATION

By using molecular dynamics models, we examine liquid droplets under various surface conditions (i.e., nanostructure configurations, surface chemistry, temperature, and electrical potential) to estimate contact angles as a measure of wetting properties [9-10-11-12]. Once a droplet is placed on a surface [13], capillary forces from the contact between the liquid and the solid substrate drives the interface between the liquid and gas phases into equilibrium. In this process, the droplet at the equilibrium state allows us to measure the contact angle between the liquid-solid and liquid-vapor interlines [14]. In order to measure contact angles for varying energy well depth, a droplet containing 1500 water molecules is placed on a flat copper surface at a constant temperature of 300 K in a simulation cell with a size of 18.07 nm × 18.07 nm × 16.55 nm, as illustrated in Figure 1 insets. A copper surface is created with a face centered cubic (FCC) crystal structure where the lattice orientations are [100], [010], and [001] along x, y, and z directions, respectively, where the lattice constant is 3.615 Å. The copper surface is assumed to be completely smooth without rough structures. In each simulation model, the static contact angle of water droplet is calculated for varying energy well depth ε, i.e., varying interaction energy in the Lennard-Jones 12-6 potential [15-16]. As the interaction potential increases, the droplet's contact angle decreases, expressed by the correlation: contact angle (CA) = – 95.68C + 192.81 as plotted in Figure 1, where C is the scaling constant for energy well depth. Therefore, the modified energy well depth is ϵ'=C ϵ_{Cu} in each computation, the scaling factor varying from 1 to 2 is multiplied by the original value of ε to account for varying potential between solid atoms and oxygen atoms in each water molecule. As the energy depth increases, the contact angle linearly decreases, and the surface becomes more hydrophilic. The changes in the energy depth will affect the water droplet's shape. For example, higher values of potential lead to flat droplets whereas smaller values result in spherical shape of droplets.

This correlation enables us to further estimate the appropriate value of ε with a given contact angle measured in order to investigate thin-film evaporation. This observation shows a good agreement with previous experiments that have investigated static contact angles on various surfaces [17].

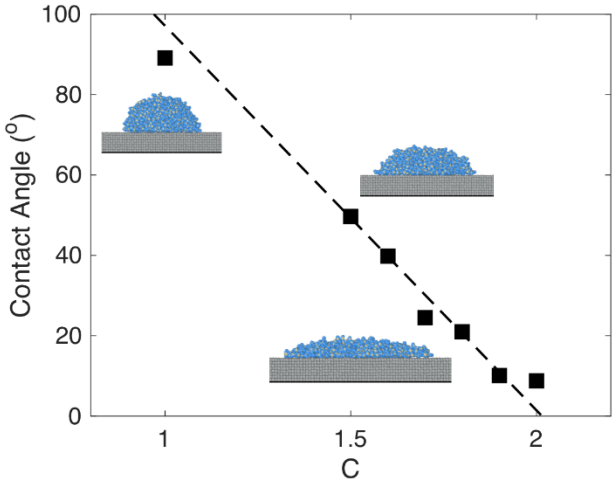

Fig. 1 Contact angle (CA) of a water droplet containing 1500 water molecules for varying energy well depth. The contact angle decreases linearly with the energy well depth such that $CA = -95.68C + 192.81$ where C is the scaling constant.

THIN-FILM EVAPORATION

We study evaporation phenomena using thin films on a flat copper surface with the aim of investigating the effects of thin-film thickness on evaporation rates. The liquid film thickness is an effective parameter in determining the equilibrium shape of the liquid menisci on various surfaces [18-19] and also evaporative performance. As the liquid film thickness changes the characteristic distance at which the molecules' interactions are behaving in favor of or against phase change varies. In this work, the atomistic scale behavior of water molecules in a thin film on a flat surface [20] is investigated to study how water molecules depart the liquid-dominated phase to vapor-dominated phase by using molecular dynamics models. We use three different liquid film thicknesses to investigate how the liquid film behaves under evaporation conditions. These studies can further help us to create the initial configuration of a thin liquid film on various engineered surfaces [21-23].

METHOD

The simulations are conducted using LAMMPS (Large-scale Atomic/Molecular Massively Parallel Simulator) [24], which is a classical molecular dynamics simulation code designed to efficiently run calculations on parallel computers. LAMMPS integrates Newton's equations of motion for a number of atoms or molecules, by computing various intermolecular forces. In this process, LAMMPS creates a list of neighboring molecules. The list is updated and further optimized for systems with particles that are repulsive at short distances, preventing a packed liquid molecule in a small volume. One of the most famous potentials to describe the potential energy of interactions between two non-bonding atoms or molecules is the Lennard Jones potential. The intermolecular interactions between water and copper molecules are modeled by the Lennard-Jones 12-6 potential [16], which can be expressed as:

$$\Phi(r) = 4\epsilon\left[\left(\frac{\sigma}{r}\right)^{12} - \left(\frac{\sigma}{r}\right)^{6}\right]$$

where r is the inter-particle distance, and σ is the length scale.

The potential used for water [25] in the current study is the TIP4P potential, developed in 1983, that has been widely used to represent water molecules. The difference between the TIP4P model and the other water models is that the site of negative charge is moved off the oxygen to a point 0.15 Å along the bisector of the H-O-H angle. Evaluation of an intermolecular interaction then requires the computation of nine or ten intermolecular distances. The single charge and two Lennard-Jones parameters for the models are optimized to reproduce the energy, density, and radial distribution functions for liquid water at 25°C.

The simulation unit cell with boundary conditions is illustrated for the case of δ_o = 1 nm in Figure 2. The simulation box is a 7.23 nm × 3.61 nm × 32.92 nm rectangular box. The initial simulation model configuration starts with a thin layer of water with a pre-defined thickness. The water film is located atop a flat copper surface. Periodic boundary conditions are applied in all directions. This will ensure particle interactions across the boundary. The simulation models consist of 3200 number of copper molecules arranged in a FCC structure with a lattice constant of 3.615 Å. Liquid films contain 870, 2610, and 4350 water molecules to represent three different thicknesses of 1 nm, 3 nm, and 5 nm, respectively. In order to reach equilibrium, the initial configuration of water film is modeled in a NVT ensemble for a period of 1 ns in a constant temperature of 300 K. The equilibrium states for three different liquid film thicknesses are shown in Figure 3.

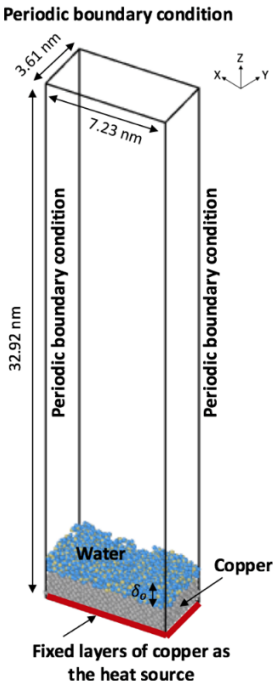

Fig. 2 Simulation unit cell for the case of δ_o = 1 nm and boundary conditions. The simulation box is a 7.23 nm × 3.61 nm × 32.92 nm rectangular box. Periodic boundary conditions are applied in all directions. Two layers of copper at the bottom are fixed and defined as a heat source by possessing a higher temperature.

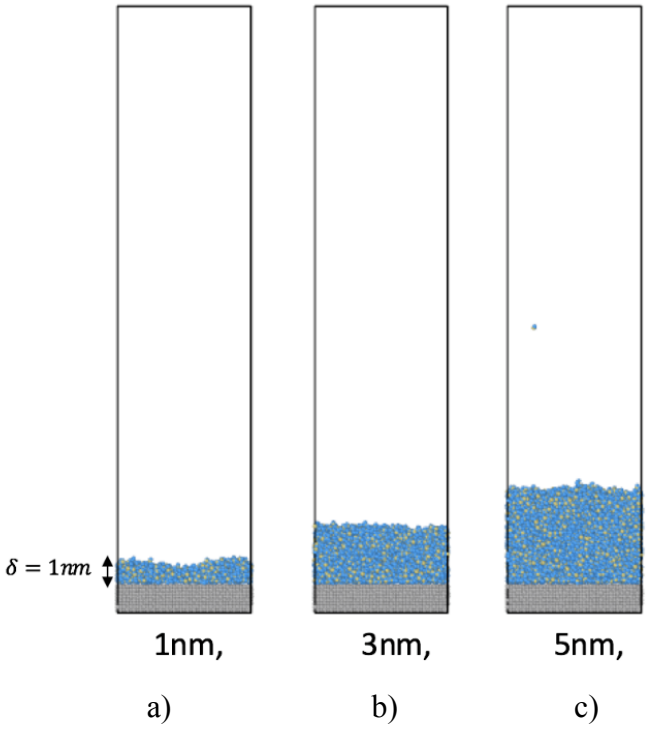

Fig. 3 Simulation cells after the equilibrium state for different thin-film thicknesses. As the initial configuration, a rectangular layer consisting of water molecules is placed on a flat copper surface, and the liquid is then equilibrated for 1 ns. Thickness of the water film is: a) 1 nm with 870 water molecules; b) 3 nm with 2610 water molecules; and c) 5 nm with 4350 water molecules.

Once equilibrium has been reached, the temperature of the first two layers of copper at the bottom, as a source term, is increased from 300 K to 500 K to simulate an evaporation condition. Then, the thermos physical properties of two phases over a range of 2.5 nanoseconds are examined. In this process, thermos physical properties (i.e., density and temperature) are recorded in grids with a size of 0.2 nm × 0.2 nm in the x-z planes. The grid size determines the analysis sensitivity; The grid size should be small enough to capture accurate distributions of the desired parameters, and at the same time large enough to contain one or more molecules in each grid. Based on this grid size, density and temperature data that are collected every 10 fs are averaged over a time period of 0.5 ns (between 2ns and 2.5ns). The corresponding averaged density and temperature profiles are shown in Figure 4 and Figure 9.

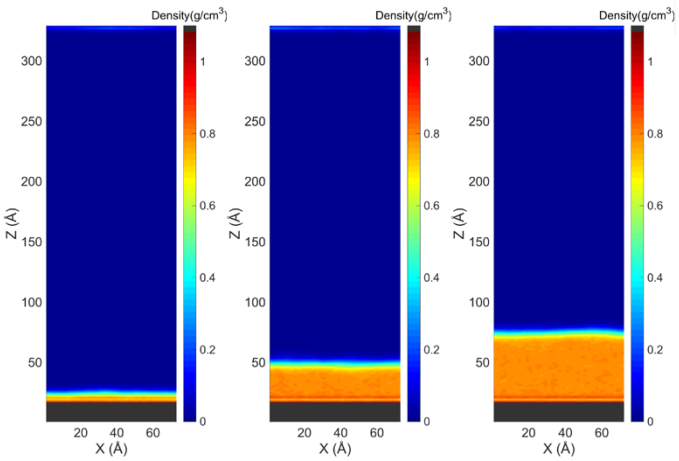

Fig. 4 Time-averaged density profiles of the thin liquid film on a flat copper surface (average values for a period of 0.5 ns between 2 ns and 2.5 ns time frames). a) 1 nm, b) 3 nm, and c) 5 nm. The values of the lower and upper density bound are used to define the density of the interface.

INTERFACE DEFINITION

Molecular dynamics simulation models provide density profiles based on the grid approach (as it is discussed in the earlier section), which can be used to distinguish between liquid or vapor phases and define the interface between two phases. The time-averaged density of each grid is calculated during a time period of 0.5 ns. While the average density is calculated as 0.8 g/cm^3 in the liquid phase and ~ 0 g/cm^3 in the vapor phase, the average value of the density of two phases can be defined as that of the liquid-vapor interface line:

$$\rho_{lv} = \frac{\rho_v + \rho_l}{2} = 0.4 \ \text{g/cm3}$$

Therefore, all the water molecules with a density larger than the liquid-vapor interfacial density, 0.4 g/cm^3, represent the liquid phase, whereas, water molecules with a density smaller than the liquid-vapor interfacial density represent the vapor phase. Therefore, the density values are plotted along the z-direction in Figure 5 based on the one-dimensional assumption.

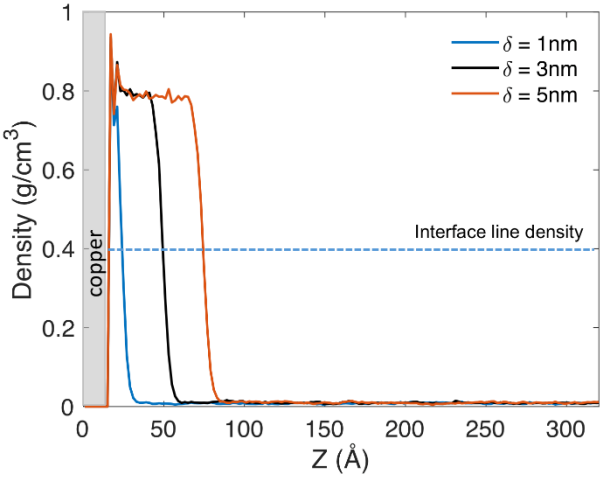

Fig. 5 Density of the water thin film along the *z*-axis after the equilibrium state. The initial thickness of the water film is 1 nm, 3 nm, and 5 nm, respectively.

EVAPORATION RATE ANALYSIS

In order to calculate the evaporation flux, first the liquid and vapor phases are defined by using the liquid-vapor interfacial density of 0.4 g/cm^3. Then, the water molecules below the liquid-vapor interface are calculated every 0.05 ns as shown in Figure 7 a, b, and c. In these figures, the number of water molecules decays rapidly at first at 0.5 - 1.5 ns and gets stabilized after ~ 1.5 ns. After the stabilization, the water molecule numbers fluctuate because while some of the water molecules depart the surface of liquid film, other water molecules in the vapor phase condense on the surface as a result of the attractive forces between the molecules. These fluctuations happen due to this continuous combination of evaporation and condensation in the system.

The time evolution of evaporation is illustrated in Figure 6, for various time frames during the simulation time. It is worth noting that during evaporation process, due to the periodic boundary conditions, some of the water molecules in the vapor phase will be condensed to the top surface, which is the opposite side of the solid surface. The evaporation flux between two time frames of t_1 and t_2 (ns) can be calculated by

$$m" = m_{H_2O}(N_{t1} - N_{t2})/A(t_2 - t_1)$$

where m" is the evaporation rate; m_{H2O} is the mass of a water molecule; N is the number of liquid water molecules; t is time; and A is the area of the flat surface of liquid film. By using three different liquid film thicknesses, evaporation rates are calculated, as shown in Figure 8 where t_1 and t_2 are the lower and upper bounds of the selected time frames, respectively. In this plot, as the liquid film thickness increases from 1 to 3 nm, the evaporation rate increases from 110-120 kg/m^{2}s.

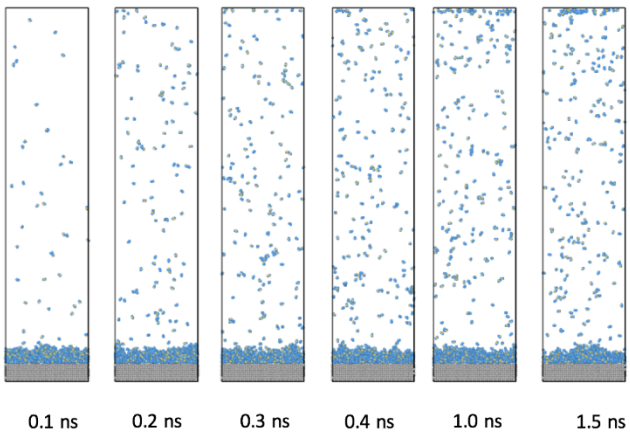

Fig. 6 Time-evolving captures showing thin-film evaporation on a flat copper surface with δ_o=1 nm. After about 1 ns, the number of water molecules departing the interface is comparable to the number of molecules condensing at the interface, resulting in the stabilized interface.

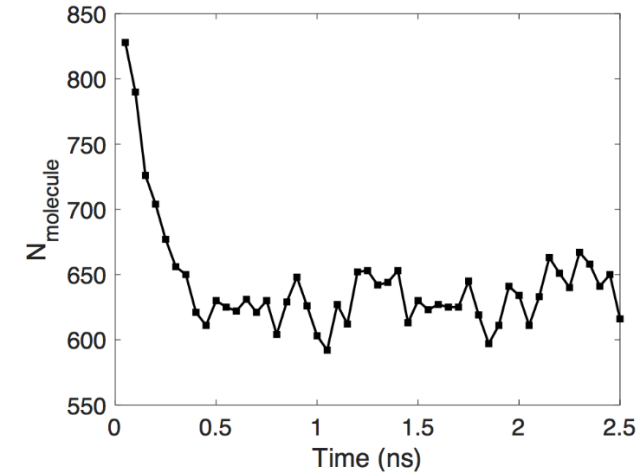

a)

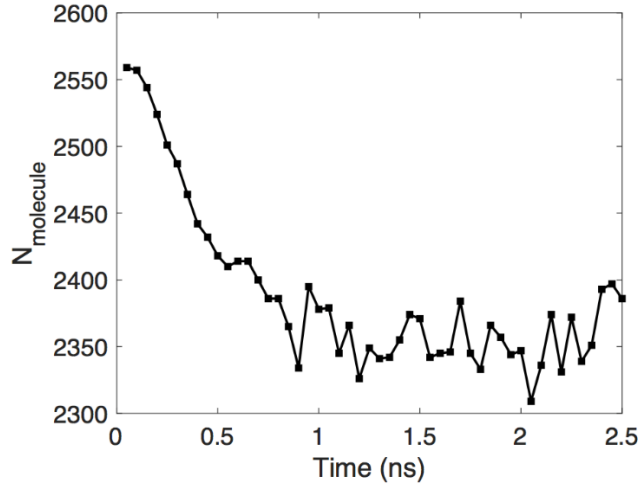

b)

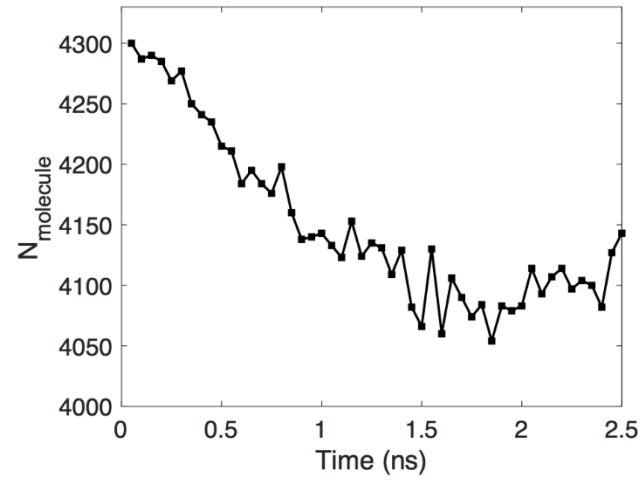

c)

Fig. 7 Variations of the number of molecules in the liquid film during the evaporation process: a) 1 nm, b) 3 nm, and c) 5 nm thick liquid films. Fluctuations after 1 ns are attributed to the continuous combination of evaporation and condensation in the system.

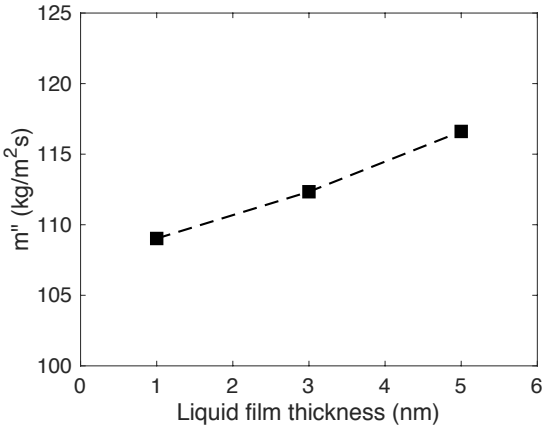

Fig. 8 Evaporation rate as a function of liquid film thickness. The trend shows an increase in evaporation rate as the liquid film thickness increases.

TEMPERATURE CALCULATION

It is important to understand the temperature information of the system during evaporation in order to calculate the heat flux between liquid-vapor phases as a next step. We identify temperature in the two-phase system by using the expression for kinetic temperature:

$$K_e = \frac{F}{2}kT$$

where K_e is the total kinetic energy for all the atoms in the grid; F is the total number of degrees of freedom for all the atoms in the grid; k is the Boltzmann constant which is equal to 1.3807×10^{-23} , and T is the temperature. Water molecules originally have 9 degrees of freedom in vibrational, rotational, and translational directions of motion. The SHAKE algorithm is used to apply bond and angle constrains to the bonds and angles of water molecules such that the water molecules become rigid and the vibrational motions are prevented. Therefore, for the TIP4P water model, the degrees of freedom of water molecules are reduced to 6 for water molecules in translational and rotational movements.

The temperature based on the kinetic energy model can be calculated from molecular dynamics using a grid approach, as explained earlier. The representative temperature maps are shown in Figure 9. Temperature data is collected every 10 fs and averaged over a time period of 0.5 ns from 2 ns to 2.5 ns. As shown in Figure 9, the vapor temperature ranges from almost 400 K to local hot spots at 600 K, and the mean temperature of the evaporating liquid phase is lower than that of vapor phase while the temperature of the copper substrate is maintained at 500 K. Uneven distribution of temperature in the vapor phase is a result of the stochastic nature of the calculation method whereas the temperature distribution in solid or liquid phases is relatively uniform.

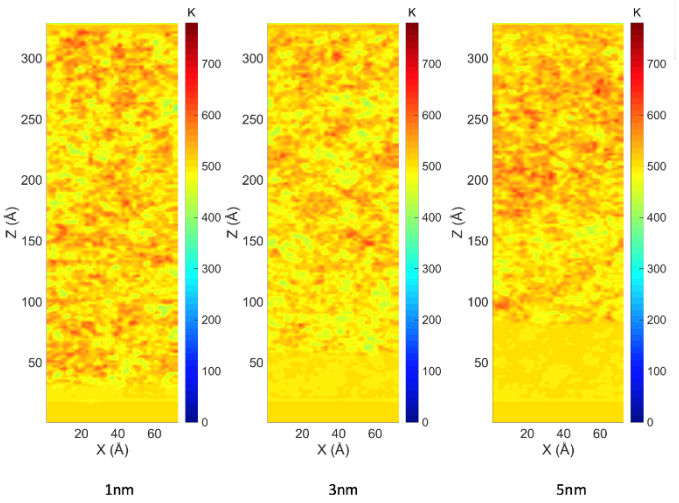

Fig. 9 Time-averaged temperature maps for a time period of 0.5 ns (from 2.0 ns to 2.5 ns) by averaging the collected data every 10 fs. Mean temperature of liquid phase is lower than that of vapor phase. The nonuniform distribution of temperature in the vapor phase is due to the probability of the grid being empty at some time frames and being filled in other time frames.

CONCLUSION

In this study, we investigate the behavior of an evaporating thin water film on copper flat surfaces using atomistic-level calculations. The molecular dynamic method applied in this work is capable of simulating particles' behavior and their interactions based on numerical algorithms that account for interatomic forces between particles. By using appropriate interatomic potentials, simulation models estimate how liquid-solid contact lines form on various substrates and liquid-vapor interfaces evolve during phase change processes. Also, detailed information on the evolution of phase change process accompanied by precise data on density and temperature distributions can be obtained. These calculations will provide time-averaged evaporation rates for different thin-film thicknesses. The understanding gained from this study will enable us to classify evaporating regimes along with liquid-vapor interface during equilibrium, and thin-film evaporation. This study will further provide guidance in selecting appropriate design parameters for better evaporation and microelectronic cooling devices.

ACKNOWLEDGMENT

This work was sponsored by the National Science Foundation (NSF), (CBET-TTP 1643347, Dr. Jose Lage, the Program Director, Thermal Transport Processes). K.M. is thankful for the financial support from the UCI Mechanical and Aerospace Engineering Department Graduate Fellowship.

REFERERENCES

[1] Dang, Liem X., and Tsun-Mei Chang. "Molecular dynamics study of water clusters, liquid, and liquid–vapor interface of water with many-body potentials." The Journal of chemical physics 106, no. 19 (1997): 8149-8159.

[2] Taylor, Ramona S., Liem X. Dang, and Bruce C. Garrett. "Molecular dynamics simulations of the liquid/vapor interface of SPC/E water." The Journal of Physical Chemistry 100, no. 28 (1996): 11720-11725.

[3] Trokhymchuk, Andrij, and José Alejandre. "Computer simulations of liquid/vapor interface in Lennard-Jones fluids: Some questions and answers." The Journal of chemical physics 111, no. 18 (1999): 8510-8523.

[4] Townsend, R. Michael, and Stuart A. Rice. "Molecular dynamics studies of the liquid–vapor interface of water." The Journal of chemical physics 94, no. 3 (1991): 2207-2218.

[5] Nijmeijer, M. J. P., A. F. Bakker, C. Bruin, and J. H. Sikkenk. "A molecular dynamics simulation of the Lennard-Jones liquid–vapor interface." The Journal of chemical physics 89, no. 6 (1988): 3789-3792.

[6] Maroo, S.C. and Chung, J.N., 2013. A possible role of nanostructured ridges on boiling heat transfer enhancement. Journal of Heat Transfer, 135(4), p.041501.

[7] Yang, T. H., and Chin Pan. "Molecular dynamics simulation of a thin water layer evaporation and evaporation coefficient." International journal of heat and mass transfer 48, no. 17 (2005): 3516-3526.

[8] Maroo, Shalabh C., and J. N. Chung. "Molecular dynamic simulation of platinum heater and associated nano-scale liquid argon film evaporation and colloidal adsorption characteristics." Journal of colloid and interface science 328, no. 1 (2008): 134-146.

[9] Thompson, S. M., K. E. Gubbins, J. P. R. B. Walton, R. A. R. Chantry, and J. S. Rowlinson. "A molecular dynamics study of liquid drops." The Journal of chemical physics 81, no. 1 (1984): 530-542.

[10] Beckstein, Oliver, and Mark SP Sansom. "Liquid–vapor oscillations of water in hydrophobic nanopores." Proceedings of the National Academy of Sciences 100, no. 12 (2003): 7063-7068.

[11] Rafiee, Javad, Xi Mi, Hemtej Gullapalli, Abhay V. Thomas, Fazel Yavari, Yunfeng Shi, Pulickel M. Ajayan, and Nikhil A. Koratkar. "Wetting transparency of graphene." Nature materials 11, no. 3 (2012): 217-222.

[12] Raj, Rishi, Shalabh C. Maroo, and Evelyn N. Wang. "Wettability of graphene." Nano letters 13, no. 4 (2013): 1509-1515.

[13] Vo, T.Q. and Kim, B., 2016. Transport phenomena of water in molecular fluidic channels. Scientific reports, 6.

[14] Sharma, S. and Debenedetti, P.G., 2012. Evaporation rate of water in hydrophobic confinement. Proceedings of the National Academy of Sciences, 109(12), pp.4365-4370.

[15] Sidorenkov, Alexander V., Sergey V. Kolesnikov, and Alexander M. Saletsky. "Molecular dynamics simulation of graphene on Cu (111) with different Lennard-Jones parameters." The European Physical Journal B 89, no. 10 (2016): 220.

[16] Sarkar, Suranjan, and R. Panneer Selvam. "Molecular dynamics simulation of effective thermal conductivity and study of enhanced thermal transport mechanism in nanofluids." Journal of applied physics 102, no. 7 (2007): 074302.

[17] Kandlikar, S.G. and Steinke, M.E., 2002. Contact angles and interface behavior during rapid evaporation of liquid on a heated surface. International Journal of Heat and Mass Transfer, 45(18), pp.3771-3780.

[18] Hens, Abhiram, Rahul Agarwal, and Gautam Biswas. "Nanoscale study of boiling and evaporation in a liquid Ar film on a Pt heater using molecular dynamics simulation." International Journal of Heat and Mass Transfer 71 (2014): 303-312.

[19] Hu, H., Weinberger, C.R. and Sun, Y., 2014. Effect of nanostructures on the meniscus shape and disjoining pressure of ultrathin liquid film. Nano letters, 14(12), pp.7131-7137.

[20] Natarajan, Suresh Kondati, and Jörg Behler. "Neural network molecular dynamics simulations of solid–liquid interfaces: water at low-index copper surfaces." Physical Chemistry Chemical Physics 18, no. 41 (2016): 28704-28725.

[21] Sarkar, S., Selvam, R.P., 2007, "Molecular Dynamics simulation of effective thermal conductivity and study of enhanced thermal transport mechanism in nanofluids" Journal of Applied Physics, 102(7)

[22] Akıner, T., Ertürk, H. and Atalık, K., 2013, November. Prediction of Thermal Conductivity and Shear Viscosity of Water-Cu Nanofluids Using Equilibrium Molecular Dynamics. In ASME 2013 International Mechanical Engineering Congress and Exposition (pp. V08CT09A012-V08CT09A012). American Society of Mechanical Engineers.

[23] Mao, Y. and Zhang, Y., 2013, July. Molecular Simulation on Explosive Boiling of Water on a Hot Copper Plate. In ASME 2013 Heat Transfer Summer Conference collocated with the ASME 2013 7th International Conference on Energy Sustainability and the ASME 2013 11th International Conference on Fuel Cell Science, Engineering and Technology (pp. V001T03A012-V001T03A012). American Society of Mechanical Engineers.

[24] Parks, Michael L., Pablo Seleson, Steven J. Plimpton, Stewart A. Silling, and Richard B. Lehoucq. "Peridynamics with LAMMPS: A User Guide, v0. 3 Beta." Sandia Report (2011–8253) (2011).

[25] Jorgensen, W.L. and Jenson, C., 1998. Temperature dependence of TIP3P, SPC, and TIP4P water from NPT Monte Carlo simulations: Seeking temperatures of maximum density. Journal of Computational Chemistry, 19(10), pp.1179-1186.